Bull Earthquake Eng (2014) 12:2211–2230
DOI 10.1007/s10518-014-9628-7

ORIGINAL RESEARCH PAPER

# The role of site effects in the comparison between code provisions and the near field strong motion of the Emilia 2012 earthquakes

**Maria Rosaria Gallipoli · Leonardo Chiauzzi · Tony Alfredo Stabile · Marco Mucciarelli · Angelo Masi · Carmine Lizza · Luigi Vignola**

Received: 30 January 2013 / Accepted: 20 April 2014 / Published online: 7 May 2014


**Abstract** A damaging seismic sequence hit a wide area mainly located in the Emilia-Romagna region (Northern Italy) during 2012 with several events of local magnitude $M_l \geq 5$, among which the $M_l$ 5.9 May 20 and the $M_l$ 5.8 May 29 were the main events. Thanks to the presence of a permanent accelerometric station very close to the epicentre and to the temporary installations performed in the aftermath of the first shock, a large number of strong motion recordings are available, on the basis of which, we compared the recorded signals with the values provided by the current Italian seismic regulations, and we observed several differences with respect to horizontal components when the simplified approach for site conditions (based on Vs30 classes) is used. On the contrary, when using the more accurate approach based on the local seismic response, we generally obtain a much better agreement, at least in the frequency range corresponding to a quarter wavelength comparable with the depth of the available subsoil data. Some unresolved questions still remain, such as the low frequency behaviour ($<1$ Hz) that could be due either to complex propagation at depth larger than the one presently investigated or to near source effects, and the behaviour of vertical spectra whose recorded/code difference is too large to be explained with the information currently available.

**Keywords** Emilia earthquake · Strong motion · Site effects · Pseudoacceleration spectrum · Housner Intensity

M. R. Gallipoli (✉) · T. A. Stabile
National Research Council - IMAA, Tito, Italy
e-mail: mariarosaria.gallipoli@imaa.cnr.it

L. Chiauzzi · M. Mucciarelli · A. Masi
School of Engineering, University of Basilicata, Potenza, Italy

M. Mucciarelli
CRS-OGS, National Institute of Oceanography and Experimental, Trieste, Italy

C. Lizza · L. Vignola
Mallet s.r.l, Marsicovetere, PZ, Italy

## 1 Introduction

On May 20, 2012 at 04:03:52 a.m. local time, a magnitude $M_l$ 5.9 ($M_w$ 6.1) earthquake with a shallow focal depth (6.3 km) occurred in the Emilia Romagna region (Northern Italy). This event started a long sequence with seven $M_l \geq 5$ earthquakes including a strong shock $M_l$ 5.8 ($M_w$ 6.1) on May 29, 2012. The earthquake caused heavy damage in several villages mainly located in Emilia, where Mercalli-Cancani-Sieberg (MCS) intensity values ranging from V to VII-VIII degree were observed. Figure 1 (from Galli et al. 2012) reports the epicentre and the focal mechanism of the strongest shocks of the sequence superimposed to the map of the cumulative intensity.

Historical seismicity shows that the mainly affected area was not struck by earthquakes with an epicentral intensity higher than $I_{MCS} = VI$. The strongest historical event, occurred in Ferrara, about 30 km away from the area mainly involved in the 2012 sequence, on November 17, 1570 with a maximum intensity equal to $I_{MCS} = VII–VIII$. Also in that case, there was a long sequence with several mainshocks followed by a series of significant aftershocks which went on until 1572.

In the aftermath of the first shock of May 20, 2012, several research groups installed temporary seismometric and accelerometric networks providing a large number of strong motion recordings. The occurrence of the last earthquakes (Abruzzo and Emilia earthquakes,

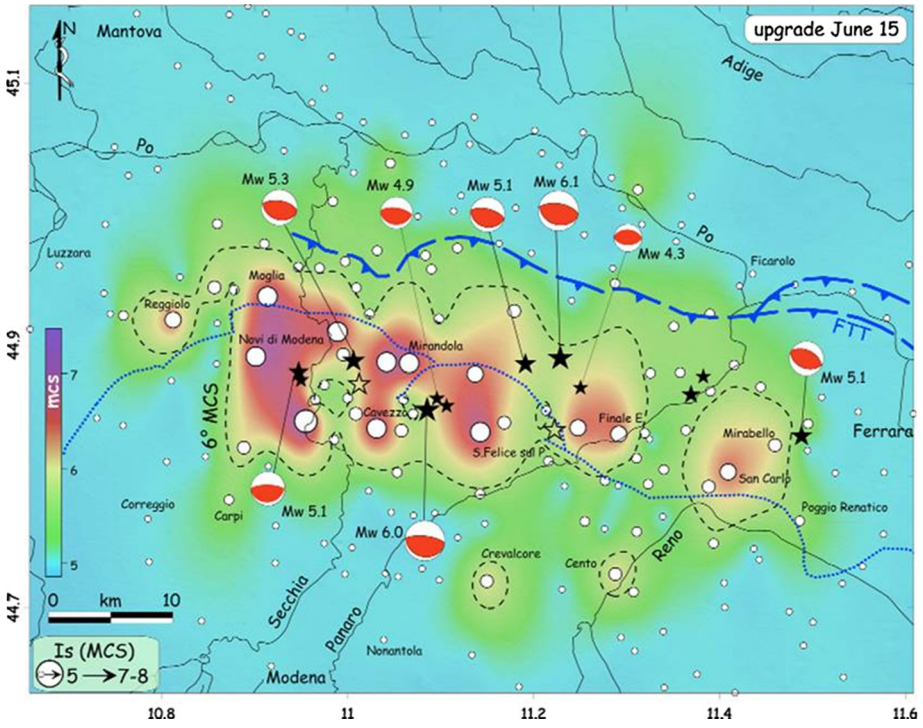


**Fig. 1** Intensity data point distribution of the Emilia sequence from May 20 to June 3, 2012. *White circles* are proportional to MCS degrees. The *background image* indicates the areal shaking in MCS terms. *Dashed line* is the interpolated VI MCS isoseismal; *dashed blue line* is the buried front of Ferrara thrusts to which the focal mechanisms of the most intense quake are referred (from Galli et al. 2012)

e.g. Masi et al. 2011a for Abruzzo quake) gave us the opportunity to compare the recorded peak, spectral and integral parameters (Housner Intensity) with the values provided by the NTC-2008 Italian Code (NTC 2008).

As already discussed in Masi et al. (2011a), although the hazard map cannot be validated or refuted on the basis of a single earthquake, a comparison with real strong motion data gives a valuable opportunity. Indeed, even remaining in the classic frame of probabilistic seismic hazard analysis (PSHA), such comparisons allow to analyse and possibly update the data on which the approach is based, as well as the selection of the ground motion parameters adopted in defining the hazard map.

The NTC-2008 Italian building code includes the hazard map based on the definition of site-dependent elastic spectra at each site of a dense grid covering the whole Italian territory (Stucchi et al. 2011). Starting from the uniform hazard spectrum (UHS) provided by the PSHA the spectral shapes of NTC08 (code spectra) are based on three parameters for each return period: the peak ground acceleration (PGA) and two additional parameters that allow the spectral shape to more closely fit the UHS, that is the corner period and the spectral amplification factor (see Montaldo et al. 2007 and Stucchi et al. 2011 for more details).

In order to take the site effects into account two different approaches are proposed in the NTC-2008 code. Particularly, the simplified approach provides the use of spectral amplification factors proportional to different soil categories taking into account the stratigraphic (SS, based on Vs30) and topographic (ST) conditions, and a more detailed approach based on the study of the local seismic response (LSR).

In this study, the two above-mentioned approaches have been applied and the results have been compared with the recorded signals for the strongest earthquakes of the sequence ($M_l$ 5.8 and 5.9). The role of site effects is particularly important in this area due to the presence of a deep and soft soil typical of the Po Valley which induces complex wave propagation. Previous works evaluated the role of Po Valley sediments in the LSR, comparing the recorded and the code provision values (e.g.Priolo et al. 2012; Bordoni et al. 2012). The deep soil condition is the worst aspect described in the Vs30 approach site classification adopted by the Italian NTC-2008 seismic code (Gallipoli and Mucciarelli 2009). It is worth noting that the NTC-2008 code actually states that the local site response studies should be performed and that the spectra related to Vs30 classes could be used as a simplified approach, but without giving indications about when this could be done.

## 2 Seismological, geophysical and geotechnical measurements

The National Accelerometric Network (RAN) managed by the Italian Department of Civil Protection recorded a great deal of accelerometric data during the 2012 Emilia earthquake sequence. The nearest accelerometric station managed by the RAN (code MRN) was located in the town of Mirandola at a small distance from the epicentres of the two main earthquakes of the sequence that are $M_l = 5.9$ and $M_l = 5.8$, occurred on May 20 and 29, respectively.

Additionally, on the same site, temporary stations were installed in order to acquire further seismic signals. Particularly, after the event occurred on May 20, 2012 three accelerometric stations were installed: two for the monitoring of the hospital service centre of Mirandola (see Masi et al. 2013) and the other near the MRN permanent station of the National Accelerometric Network.

The accelerometers installed are ETNA-Kinemetrics in stand-alone configuration with local data storage. The data were recorded at 100 sps. While the MRN station is located inside the ground level of a small building (electrical substation of the power company


**Fig. 2** Locations of accelerometric stations and single station noise measurements (*yellow*), ESAC array (*blues*) and down-hole and cross-hole tests (*red*)

ENEL), the other two stations were located in free-field respectively at 5 m from the ENEL substation (code MIRE) and inside an underground vault hosting the gas main valve of the local hospital (code MIRH).

In order to characterise the area from a geophysical standpoint, two-dimensional passive seismic arrays were performed with the aim of being processed with the extended spatial autocorrelation (ESAC) technique jointly inverted with horizontal-to-vertical spectral ratios (HVSR or H/V) to determine shear wave velocity profiles. Figure 2 reports the locations of accelerometric stations, ESAC array and single station noise measurements.

The passive array data were collected using a 24 vertical 4.5 Hz Geospace geophones, arranged in an L-shaped array with an inter-distance ranging from 1 to 60 m and the longest arm 250 m long. The data were collected using a 24 bit A/D digitiser (Geode Geometrics) with a 125μs sampling rate. The single station noise data were collected with a 24 bit tromograph (Micromed-Tromino) with 128 sps. The data analysis was performed with the ESAC code for the 2-D array (Okada 2003; Ohori et al. 2002; Parolai et al. 2006) and following the standard for the HVSR analysis given by SESAME (2004). The joint inversion was performed using the genetic algorithm approach described in Albarello et al. (2011). These analyses were performed both for MIRH and the MIRE site. Very close to MIRE and MRN stations a 30-m deep down-hole and deeper cross-hole tests were performed too. Taking advantage of the drilling for the down-hole test it was possible to retrieve a detailed stratigraphy for the surface layers as well as to take two undisturbed soil samples which were later analysed in a geotechnical laboratory to characterize shear modulus degradation and the damping of the principal lithologies, sand and clay. The result of the geotechnical and geophysical survey will be described more in depth in the section devoted to the modelling.

## 3 Analysis of recorded data and comparison with code provisions

Table 1 reports some of the maximum ground motion parameters of the data recorded during the $M_l = 5.9$ (May 20, 2012) and $M_l = 5.8$ (May 29, 2012) events on the site of Mirandola by the RAN (for both the events) and temporary stations (only for the event of May 29, 2012). Specifically, the values of PGA, peak ground velocity (PGV) and peak ground displacement (PGD) are reported for the three components (horizontal: NS and EW; vertical: UP). All the uncorrected data (both ours and those of RAN) were processed using a linear baseline correction and filtered using a Butterworth 4th-order filter with a bandpass 0.1–25 Hz.

As it has already been stated, analyses and comparisons in terms of peak values provide a clear reading of earthquake ground motion through parameters commonly used in seismic

**Table 1** PGA, PGV, PGD and $I_H$ for each component recorded at the MRN-RAN, MIRE and MIRH stations for the main seismic events occurred on May 20 and 29, 2012

| EVENT | Station code | Epic. distance (km) | Component | PGA (g) | PGV (cm/sec) | PGD (cm) | $I_H$ (cm) |
|---|---|---|---|---|---|---|---|
| 5.9 Ml May 20, 2012 | MRN | 13.4 | NS | 0.29 | 40.00 | 10.71 | 129 |
| | | | EW | 0.28 | 32.43 | 6.28 | 84 |
| | | | UP | 0.32 | 5.65 | 1.26 | 17 |
| 5.8 Ml May 29,2012 | MRN | 3.6 | NS | 0.29 | 40.07 | 19.77 | 135 |
| | | | EW | 0.23 | 23.62 | 9.21 | 70 |
| | | | UP | 0.87 | 22.71 | 5.70 | 31 |
| | MIRE | 3.6 | NS | 0.30 | 40.45 | 19.94 | 136 |
| | | | EW | 0.18 | 24.30 | 8.93 | 69 |
| | | | UP | 0.71 | 20.93 | 5.79 | 32 |
| | MIRH | 3.9 | NS | 0.30 | 48.72 | 21.76 | 117 |
| | | | EW | 0.15 | 19.25 | 5.20 | 59 |
| | | | UP | 0.52 | 16.01 | 4.96 | 29 |

design. Nevertheless, peak parameters give alone a poor description of potential ground motion severity. As an alternative to peak parameters (PGA, PGV and PGD), some studies (e.g. Decanini et al. 2002; Masi et al. 2011b) demonstrated that Housner Intensity $I_H$ (Housner 1952) can be an effective parameter to correlate the severity of seismic motions to structural damage, particularly in cases of existing non-ductile Reinforced Concrete (RC) buildings. For this reason we also computed $I_H$ defined as the area under the pseudo-velocity response spectrum ($S_v$), as shown in Eq. (1):

$$I_H = \int_{T\inf}^{T\sup} S_v(T, \xi)\, dT \tag{1}$$

where T is the fundamental period of the structure under examination, ξ is the damping ratio (assumed equal to 5 % in the analyses developed in this article), $T_{inf}$ and $T_{sup}$ define the interval of period values where ordinary buildings can be mostly placed. With regard to the computation of $I_H$, as already reported by Masi et al. (2011b), it is worth noting that it is usually computed in the period range [0.1–2.5] s, while in the present work the period range [0.2–2] s has been used, in accordance with the choice adopted in the studies carried out for the previous seismic classification of the Italian territory proposed by the GNDT Working Group (1999).

For the event occurred on May 20, 2012 the recorded data show high values of PGA, comparable for all the three components, that are about 0.3 g (Table 1). Particularly, the highest PGA value has been found on the vertical component (0.32 g). On the contrary, when processing the tri-axial time histories in terms of PGV, PGD and $I_H$, the values obtained on the vertical component (PGV = 5.65 cm/sec, PGD = 1.26 cm and $I_H$ = 17 cm) are smaller with respect to those provided on the horizontal ones for the same ground motion parameters ($PGV_{max}$ = 40.00 cm/sec, $PGD_{max}$ = 10.71 cm and $I_{Hmax}$ = 129 cm).

The same behaviour is highlighted again by the May 29, 2012 ($M_l$ 5.8) shock: the vertical component has a higher PGA value ($PGA_{max}$ = 0.87 g) than the values of horizontal components, on the contrary the other seismic parameters of vertical component ($PGV_{max}$ = 22.71 cm/sec, $PGD_{max}$ = 5.79 and $I_{Hmax}$ = 32 cm) are lower than the horizontal ones (Table 1). About the horizontal components the seismic severity provided by using PGA is confirmed also when processing the recorded signals in terms of PGV, PGD and $I_H$. This confirms, as already shown by other authors (e.g. Masi et al. 2011a, b; Chiauzzi et al. 2012), the importance to characterize the seismic signals through the use of multiple seismic parameters.

In order to make a comparison between the recorded data and seismic actions from code provisions, as already highlighted in recent papers by other authors (e.g. Chiauzzi et al. 2012; Iervolino 2012), Table 2 reports the comparison between recorded and NTC-2008 Italian (OPCM 3519 2006; NTC 2008) code provisions in terms of PGA and $I_H$. The comparison is carried out for two hazard levels corresponding to $T_R$ = 475 and $T_R$ = 2,475 years, which are significant for current design practice and not with respect to the seismic history of the Emilia territory. Specifically, $T_R$ = 475 years has been selected as representative of the reference value provided by the NTC-2008 for the design of ordinary buildings with respect to the life safety limit state, while $T_R$ = 2,475 years can be considered as an upper value being the maximum value of return period provided in the Italian hazard map. When making this kind of comparison one may think of including one or more standard deviation around the average value provided by the code for a given return period. The inclusion of standard deviation is in fact the same as considering a larger return period. In the Poissonian framework

**Table 2** Comparison, in terms of PGA and $I_H$, between recorded and NTC-2008 Italian code prevision values (for return periods equal to 475 and 2,475 years)

| Code Station | Comp. | Recorded | | NTC-2008 ITALIAN CODE | | | | | | | |
|---|---|---|---|---|---|---|---|---|---|---|---|
| | | | | $T_R = 475$ | | $T_R = 2,475$ | | $\%\Delta(T_R = 475)$ | | $\%\Delta(T_R = 2,475)$ | |
| | | PGA (g) | $I_H$ (cm) | PGA (g) | $I_H$ (cm) | PGA (g) | $I_H$ (cm) | Δ PGA (%) | $\Delta I_H$ (%) | Δ PGA (%) | $\Delta I_H$ (%) |
| 5.9 Ml May 20, 2012 | | | | | | | | | | | |
| MRN | NS | 0.29 | 129 | 0.21 | 64 | 0.35 | 107 | −38 | −102 | 17 | −21 |
| | EW | 0.28 | 84 | | | | | −33 | −31 | 20 | 21 |
| | UP | 0.32 | 17 | 0.07 | 6 | 0.19 | 17 | −351 | −166 | −66 | −3 |
| 5.8 Ml May 29, 2012 | | | | | | | | | | | |
| MRN | NS | 0.29 | 135 | 0.21 | 64 | 0.35 | 107 | −38 | −111 | 17 | −26 |
| | EW | 0.23 | 70 | | | | | −10 | −9 | 34 | 35 |
| | UP | 0.87 | 31 | 0.07 | 6 | 0.19 | 17 | −1,125 | −384 | −351 | −88 |
| MIRE | NS | 0.3 | 136 | 0.21 | 64 | 0.35 | 107 | −43 | −113 | 14 | −27 |
| | EW | 0.18 | 69 | | | | | 14 | −8 | 49 | 36 |
| | UP | 0.71 | 32 | 0.07 | 6 | 0.19 | 17 | −900 | −400 | −268 | −94 |
| MIRH | NS | 0.30 | 117.15 | 0.21 | 64 | 0.35 | 107 | −43 | −83 | 14 | −9 |
| | EW | 0.15 | 58.81 | | | | | 27 | 8 | 56 | 45 |
| | UP | 0.52 | 29.14 | 0.07 | 6 | 0.19 | 17 | −640 | −386 | −173 | −71 |

of NTC08, a given return period corresponds to a fixed probability in a given observation period. It would be like expressing the probability of a probability, which is pointless.

According to the soil classification provided by the Italian Building Code (NTC 2008) the seismic actions on stiff soil (category A) have been amplified according to the requirements of standard for soil class C and topography class T1, taking into account the site characterization of MRN station proposed in the ITACA Project (http://itaca.mi.ingv.it/ItacaNet/). Such classification is confirmed by the data collected in this study as described in Sect. 2 and analysed in the following.

Bearing in mind the different nature of code and response spectra from real single events, it has to be emphasized at the outset that a judgement of the current Italian hazard map cannot be made from such a comparison (Masi et al. 2011a). Nevertheless, a comparison may be useful as it has been shown in other studies (e.g. Crowley et al. 2009; Iervolino et al. 2010; Gunay and Mosalam 2010). Indeed, a comparison between the spectra and ground motion parameters of recorded signals with the code provisions permits an evaluation of the relative position of the Emilia earthquakes with respect to the current distribution of PSHA. Furthermore, other valuable results can be drawn analyzing recorded data through various seismic parameters which have different capabilities of representing damage potential of ground motion time histories. In Table 2 the differences in terms of PGA and $I_H$ between code (NTC-2008) and recorded (MRN, MIRE and MIRH) values are reported, computed according to Eqs. (2) and (3):

$$\Delta PGA_{T_R} = \left[100\frac{PGA_{NTC08} - PGA_{RAN}}{PGA_{NTC08}}\right]_{T_R} \tag{2}$$

$$\Delta I_{H,\,T_R} = \left[100\frac{I_{H,\,NTC08} - I_{H,\,RAN}}{I_{H,\,NTC08}}\right]_{T_R} \tag{3}$$

The results in Table 2 show large differences between code values and strong motion signals recorded during the Emilia 2012. As can be seen, the highest difference is found analysing the vertical component of seismic recorded signals particularly for the event occurred on May 29, 2012. Moreover, code values provided for $T_R = 475$ years are always lower than the recorded ones, comparing them both in terms of PGA and $I_H$. The comparison with the code actions provided for $T_R = 2,475$ years shows comparable values processing data in terms of PGA, while in terms of $I_H$ the results are comparable only on the EW component, while on the NS one code values remain lower.

Figures 3 and 4 shows the comparison between recorded and code provision values in terms of pseudo-acceleration, pseudo-velocity and displacement elastic response spectra (computed using a damping ratio of 5 %), respectively for horizontal and vertical components. Particularly, the computed elastic response spectra have been compared with the ones provided by NTC-2008 Italian Code considering the return periods of 475 and 2,475 years and the soil type conditions (class C, topography T1) of the relevant stations.

The reliability of the recordings is confirmed by the fact that for the May 29 event the spectra at MIRE and MRN are practically identical, except for a mismatch around 8 Hz that could be due to the different type of equipment housing (free field for MIRE versus building basement for MNR, see Ditommaso et al. 2010 for a discussion of the influence of housing on accelerometric recordings).

The large vertical component of this earthquake has also been recognised by authors who analysed the distribution of damage due to this kind of component (Grimaz and Malisan 2013). The very large difference in vertical components will require additional analysis taking into account two factors: the proximity to the source (Mirandola is just over the fault) and a

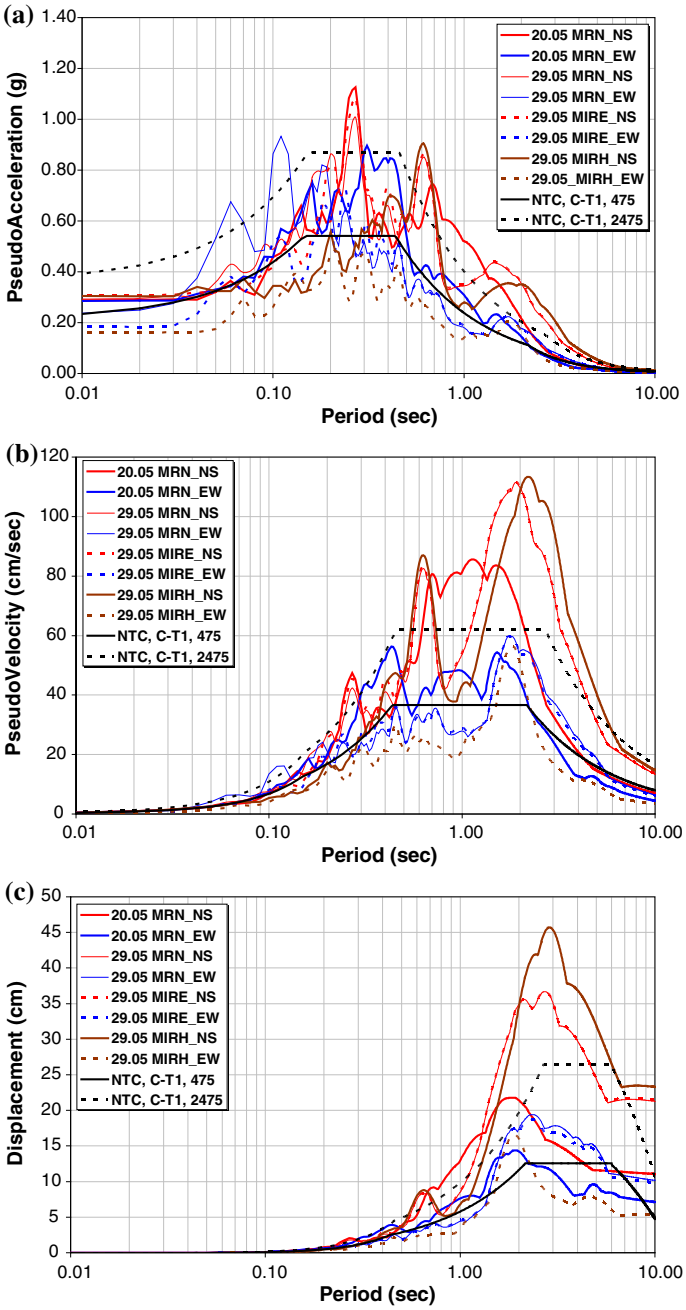


**Fig. 3** Comparison of the pseudoacceleration (**a**), pseudovelocity (**b**) and displacement (**c**) response spectra of Emilia main shocks (May 20 and 29, 2012) and of the NTC-2008 Italian Code computed at the sites of the recorded stations (MRN, MIRE and MIRH) for the return period of 475 and 2,475 years (horizontal components, NS and EW)

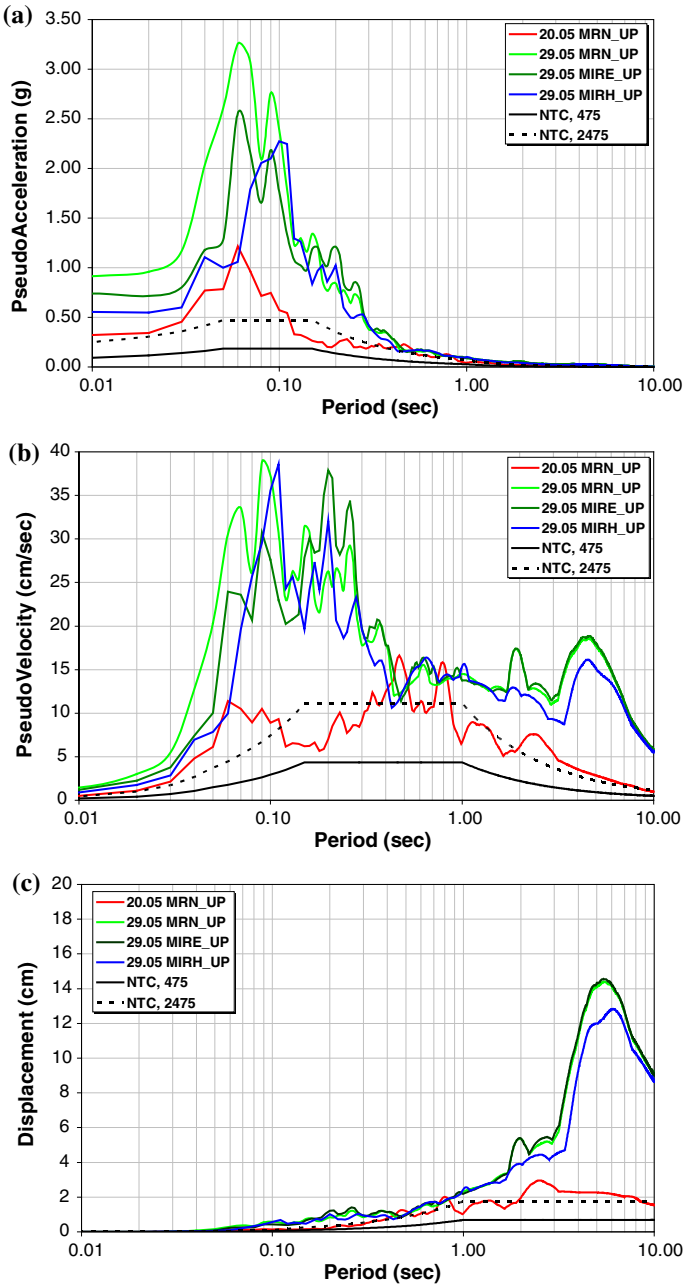


**Fig. 4** Comparison of the pseudoacceleration (**a**), pseudovelocity (**b**) and displacement (**c**) response spectra of Emilia main shocks (May 20 and 29, 2012) and of the NTC-2008 Italian Code computed at the sites of the recorded stations (MRN, MIRE and MIRH) for the return period of 475 and 2,475 years (vertical component, UP)

velocity profile to a greater depth than the 30 m now available. However, the higher differences between code and recorded values are found on the vertical component, thus suggesting to reconsider the seismic code provisions on the vertical component of the seismic action and its combination with the horizontal one.

Focusing only on the horizontal components of ground motion, very different spectra were observed at the site of Mirandola especially for the two events (May 20 and 29, 2012) and between the NS and EW components.

In terms of pseudo-acceleration response spectra $S_a(T, \xi = 5\,\%)$, when $T_R = 475$ years, the spectral values from NTC-2008 are generally lower than those from the recorded signals. For $T_R = 2,475$ years, code response spectra are comparable with those provided from the recorded signals.

Also considering the pseudo-velocity response spectra $S_v(T, \xi = 5\,\%)$, when a return period $T_R = 475$ years is considered, the spectral values from NTC-2008 are generally lower than those from the recorded signals. For $T_R = 2,475$ years, pseudo-velocity response spectra provided in NTC-2008 are comparable when EW component is considered, while they are lower comparing the NS components. In terms of spectral displacement, for both the return periods, the code values are generally lower than those from the recorded signals.

The comparisons carried out and the relevant results need further studies to better understand the differences and their significance, also considering the very different shape between code and recorded spectra. In order to quantify the difference between the shape of response spectra and the code ones, we have evaluated the integral function $I_H(T)$ of the Housner Intensity (Figure 5). The Housner Intensity has been computed according to Eq. (1) in the period range $T = [0, 4]$ s (with $\xi = 5\,\%$). Figure 5 shows that the integral function of the $I_H$ computed on the mean values of recorded signals (mean of signals recorded at MRN, MIRE and MIRH stations for the events of May 20 and 29, 2012) is comparable with the one calculated using code spectra at $T_R = 2,475$ years, rather than the one achieved at $T_R = 475$ years. It is worth noting that the relative position of the curves changes on the basis of the considered period range possibly also as a consequence of site effects, as reported in the next paragraphs.

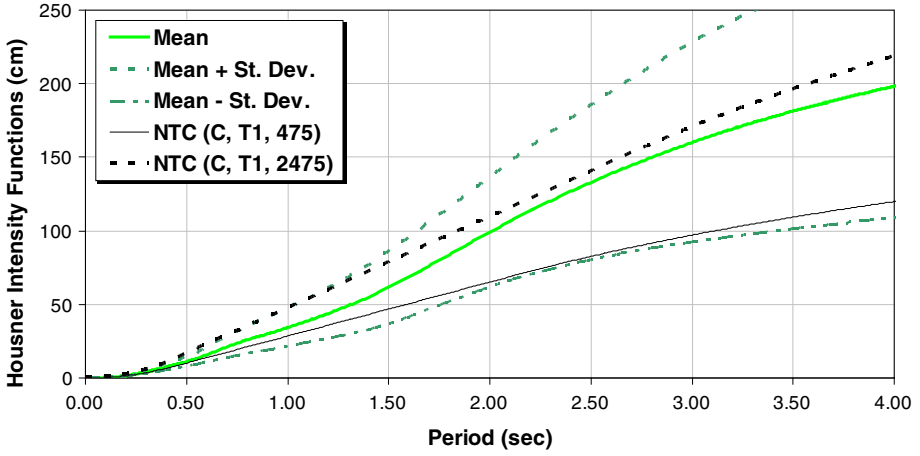


**Fig. 5** Housner intensity functions of recorded signals (mean of signals recorded at MRN, MIRE and MIRH stations for the events of May 20 and 29, 2012) compared with the *curves* computed on the pseudovelocity response spectra provided by NTC-2008 for the site Mirandola at the return period of 475 and 2,475 years (soil class C, topography T1)

As can be seen in Fig. 5, while the $I_H(T)$ computed on the mean $S_V(T)$ response spectra is well approximated to the curve computed for the action expected for the return period of 2,475 years, the lower values of the distribution are approximated by the action provided for the return period of 475 years. On the other hand, the mean values of the $I_H(T)$ distribution are much larger than the expected values for the return period of $T_R = 475$ years. By considering the mean plus the standard deviation values of the $I_H(T)$ distribution also the expected values for $T_R = 2,475$ years exceeded.

## 4 Analysis of site effect

As seen in the previous section, there is a large difference between the peak and integral parameters from code provision or recorded data. Since the area affected by the Emilia earthquake lies on soft and deep soil, we wanted to investigate whether the above mentioned difference is mainly due to the parameterisation of code spectra (shape and anchor value) or to the way site effects are accounted for. Indeed, previous works (Gallipoli and Mucciarelli 2009; Luzi et al. 2011) show that the Vs30 classification in the Italian code fails to describe correctly the real LSR on soft and deep soils. The following analyses will be described for sake of simplicity just for the MIRE station because it has the largest number of recordings available and the shear wave profile is very similar between MIRE and MIRH. At the MIRE station there are 107 recordings available with magnitude ranging between 3.0 and 5.8 and epicentral distance between 0.6 and 32.7 km.

Velocity profile from down-hole test down to 30 m and from the ESAC+HVSR inversion at a higher depth are reported in Fig. 6: the values are very similar and show three main jumps: at about 8–10 m there is a transition from clay to sand with a velocity increasing from 140 to 240 m/s; at 30 m there is a lithological variation with an increase in density and stiffness of sand, with velocity reaching 350 m/s. The ESAC+HVSR inversion returned a last impedance contrast deeper at about 90 m but with a velocity of the underlying stratum still below 600 m/s.

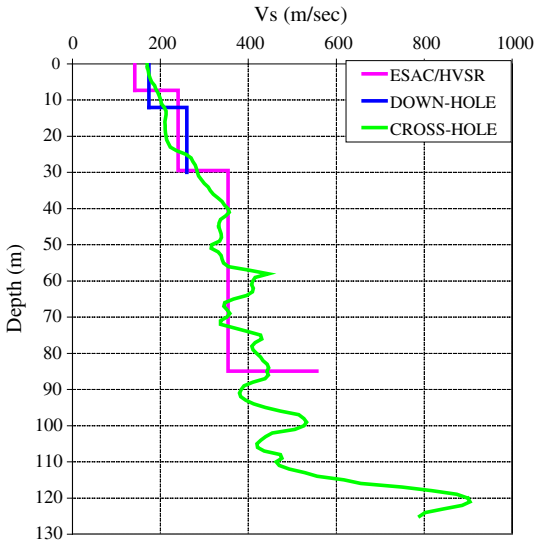


**Fig. 6** Vs velocity profiles estimated by down-hole, cross-hole and ESAC/HVSR at MIRE site

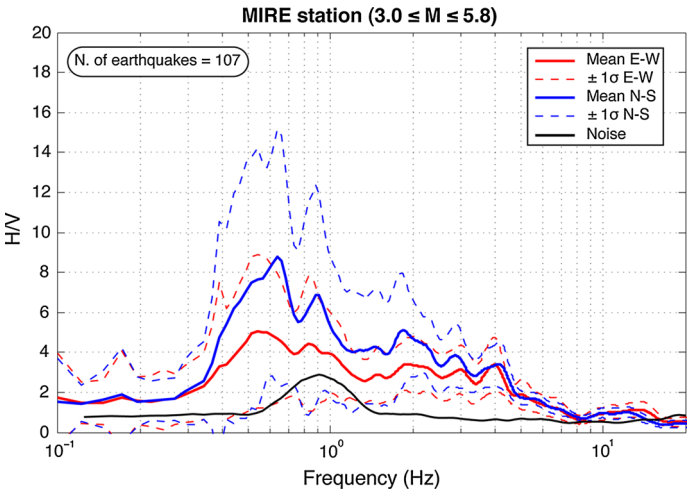


**Fig. 7** Comparison between the ambient noise HVSR curve (*black line*) and the mean HVSR curves from 107 earthquakes recordings at the MIRE station with magnitude $M_l \geq 3.0$ (*blue* and *red lines*). *Blue* and *red lines* are referred to the NS and EW components, respectively

Recently, in the framework of microzonation studies performed by the Emilia-Romagna regional government (Martelli et al. 2013) a deep cross-hole survey has been performed. Again in Fig. 6 a good agreement can be seen between the shear wave velocity profile obtained with our surface survey (ESAC+HVSR inversion) and borehole data. Moreover the cross-hole test has found the seismic bedrock with 800 m/sec at 120 m depth.

This might suggest that the resonance peak at about 0.9 Hz (∼1.1 s) is characteristic of 1-D behaviour for the sites of this area and that the three-layer model is satisfactory for simple 1-D modelling that will be described later. However, the seismic site response appears more complex when estimating HVSR obtained from the 107 recorded earthquakes. Figure 7 shows the comparison of earthquake HVSRs in the two horizontal components and the ambient noise HVSR: the difference between the ambient noise HVSR curve and the ones obtained for separate horizontal components of 107 earthquakes with $M_l \geq 3.0$ is well evident. Besides the fact that the mean NS (solid blue line) and EW (solid red line) HVSR curves are quite different, 1 σ curves are very distant from the respective mean value curves, thus indicating a large variability of the HVSR curves obtained from the earthquakes. In addition, it appears that the fundamental peak is not the one estimated at 0.9 Hz from ambient noise HVSR but a lower one at 0.6 Hz (∼ 1.7s). This difference led us to a better assessment of the large variability of earthquake HVSR curves and to investigate the resonance frequencies considering:

1. dependence on the earthquake magnitude;
2. dependence on the earthquake distance (near field effects);
3. dependence on the earthquake azimuth with respect to the recording station;

Selecting the earthquakes in different ranges of magnitude, $3.0 \leq M_l \leq 3.4$, $3.5 \leq M_l \leq 3.9$ and $4.0 \leq M_l \leq 5.8$, in all the three cases the HVSRs return the main peak at 0.6 Hz and the second one at 0.9 Hz, with peak frequency decreasing from 0.6 to 0.5 Hz for higher magnitudes (Fig. 8). Moreover, in all these cases the two component HVSRs are clearly different: the amplitude value of NS curves are always higher than the EW ones (Fig. 8).

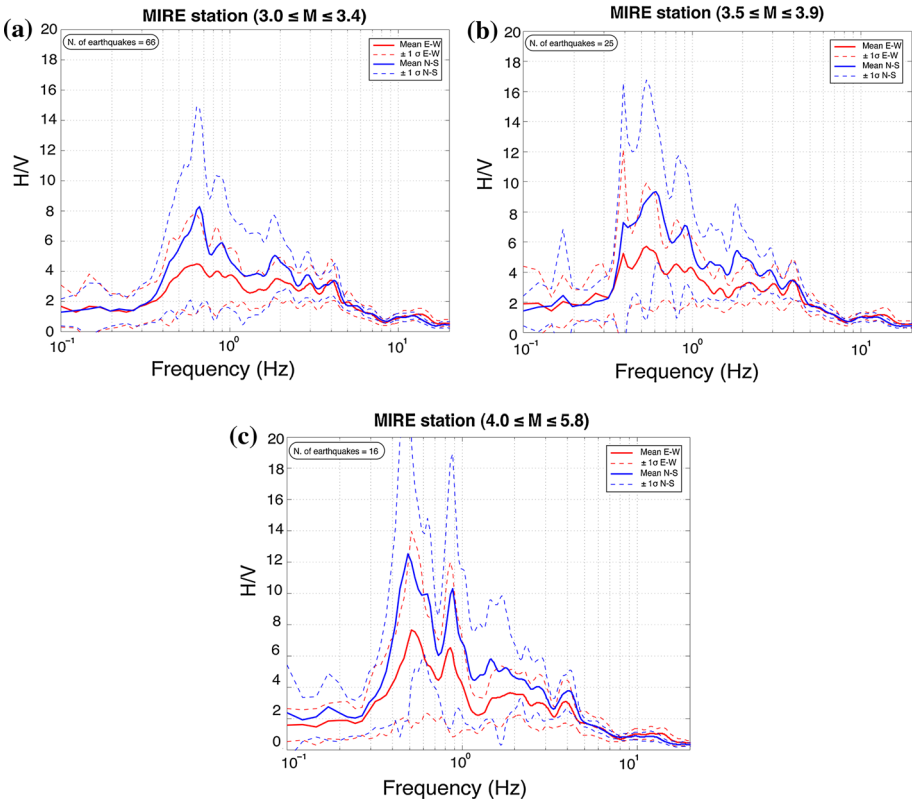


**Fig. 8** HVSR curves for earthquakes with magnitude between $3.0 \leq M_l \leq 3.4$ (**a**), $3.5 \leq M_l \leq 3.9$ (**b**) and $4.0 \leq M_l \leq 5.8$ (**c**)

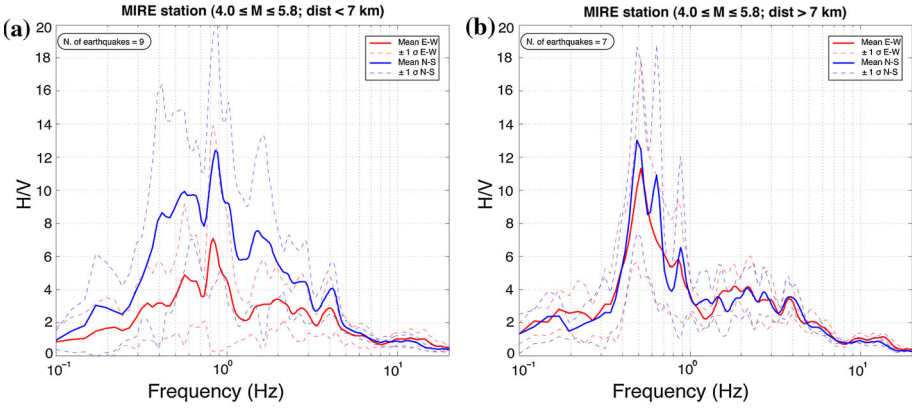


**Fig. 9** HVSR curves for earthquakes with magnitude between $M_l = 4.0$ and $M_l = 5.8$, and with epicentral distance from the MIRE station in the range 0–7 km (**a**) and 7–15 km (**b**)

Secondly, we have estimated HVSR for earthquakes with the same magnitude range and a different epicentral distance. We have selected earthquakes with magnitude ranging between 4.0 and 5.8 and two classes of epicentral distance, $d < 7$ km and $d > 7$ km. Figure 9

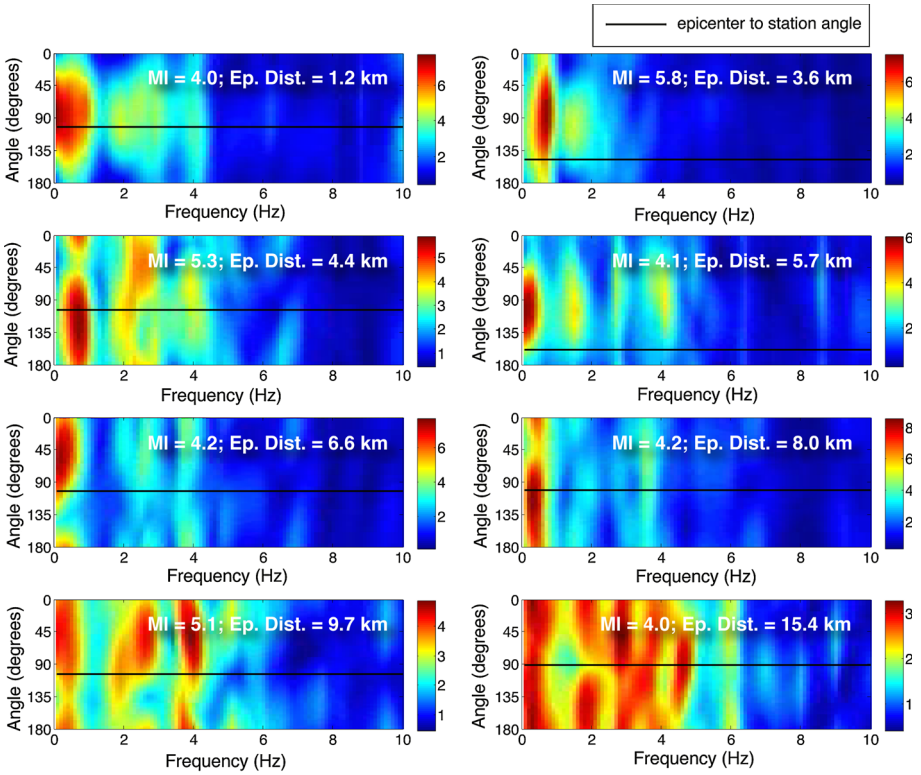


**Fig. 10** Horizontal to vertical moving angle ratios computed for $M_l > 4$ earthquakes with increasing epicentral distance. *Black horizontal line* in each panel indicates the earthquake azimuth respect to the MIRE station

shows the HVSRs for the two horizontal components: when the nine closest earthquakes are selected, the HVSR returns the main peak at 0.9 Hz (Fig. 9a) and large differences still remain between the two components of the HVSR, while when we consider more distant earthquakes the fundamental frequency becomes 0.6 Hz (Fig. 9b) and the difference between components is much smaller. This analysis points out the importance of interaction between ray path and subsoil structure. The different angle of incidence causes a variation in HVSR curves: the rays coming from more distant earthquakes highlight the subsoil structure in a more efficient way than those brought about by closer earthquakes.

Finally, we have performed the analysis of azimuthal dependence of horizontal to vertical ratios to evaluate the possible correlation between directional site effect and earthquake azimuth. The analysis was performed on rotated components of horizontal motion with a step of 5°. Figure 10 reports the Horizontal to Vertical moving angle ratios analysis computed for earthquakes with $M_l > 4$ and increasing epicentral distance: each earthquake induces a clear directional site effect and, when the distance increases, the directional contribution becomes increasingly complex in frequency and azimuth but never appears correlated with source-to-receiver azimuth (black horizontal line in each panel of Fig. 10).

## 5 Comparison of recorded data with bedrock code spectra convolved with local seismic response

As can be seen in the previous section, the ground motion recorded in Mirandola shows variability in site response when studied in detail, but some common features still persist. The presence of resonance values at low frequencies, in a range compatible with the one controlled by the first hundred meters of soils, prompted for a more detailed 1-D simulation to investigate if such effects could explain the difference observed between the code spectra and the recorded values so as to compare the LSR approach with the Vs30-based one.

During the drilling to perform the above-described down-hole measurements, two undisturbed samples were collected. By making use of a resonant column test it was possible to estimate the shear modulus degradation and damping curves for increasing deformations. Figure 11 reports the shear modulus degradation and damping curves for the first clay layer (Fig. 11a) and the second sand layer (Fig. 11b). These information and the shear wave velocity profile, reported in Fig. 6, were used as input for a 1-D numerical simulation using the program STRATA (Kottke and Rathje 2008), according with the layered model reported in Table 3. Taking advantage of the capability of code STRATA in performing random variation of parameters, a 10 % variation was enabled on shear wave velocity and thickness of each layer of the model. A synthetic accelerogram was used as input ground motion, given the unavailability of recordings at close reference sites (either borehole or rock outcrop recordings). The accelerogram was generated by means of the BELFAGOR code. This program derives from an older one, PhySimque (Mucciarelli et al. 1997), based on the theoretical work by Sabetta and Pugliese (1996), which proposes the simulation of non-stationary ground motion by using predictive equations for response spectra and time-dependent frequency parameters. The code implements a two-step procedure: at first, it generates a synthetic accelerogram

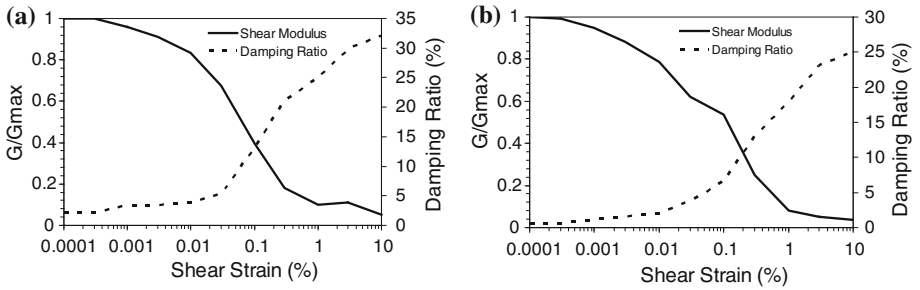


**Fig. 11** Shear modulus and damping ratio for clay (a) and sand (b) samples taken from the borehole at MIRE site

**Table 3** Mechanical characteristics for clay and sand at different levels used for 1D model of LSR

| Soil material type | Thickness of layer (m) | Maximum shear modulus Gmax (MPa) | Total unit weight (kN/m$^3$) | Shear wave velocity (m/sec) |
|---|---|---|---|---|
| Clay | 7.3 | 39.4 | 19.2 | 142 |
| Sand | 22.2 | 106.0 | 18.1 | 240 |
| Sand | 55.4 | 230.7 | 18.1 | 354 |
| Sand | 25.0 | 569.1 | 18.1 | 556 |
| Seismic bedrock | | 1,436.5 | 22.0 | 800 |

based on physical parameters (magnitude, distance and site condition) and then forces it to converge to a target response spectrum by using the recursive Fourier transformation from time-to-frequency domain and vice-versa. The target spectra selected were the NTC-2008 ones provided for the Mirandola site at 475 years of return period, for soil class A (rock) and topographic class T1 (flat surface).

When comparing code provisions and the data observed, it would be advisable to use amplification curves instead of response spectra (see e.g. Gallipoli et al. 2013 for the comparison between expected topographic amplification and observed amplification during L'Aquila, 2009, earthquake). Unfortunately, in the area of Emilia hit by the 2012 quake this is not possible because of the absence both of a reference rock site and borehole data. In the future it will be possible to overcome this difficulty thanks to an accelerometer installation foreseen below Mirandola at 150 m in depth.

Taking this limitation into account, we have compared the recorded acceleration spectra (in terms of mean and mean+standard deviation) with soil amplification coefficients (SAC) and LSR approaches. For the LSR approach we considered the distribution of 50 runs of the STRATA program, choosing the 84 % percentile to have a fair comparison with SAC: indeed, the m+sd is the standard choice for the calculation of code spectra, see the recent example provided by Pitilakis et al. (2013). Figure 12 reports the comparison between the mean and m+sd of the horizontal component response spectra of MRN, MIRE and MIRH recordings for the events of May 20 and 29, 2012 (8 recordings in total) and the code-complying spectra computed for the return periods of 475 years, using both the SAC and LSR approaches. The recorded acceleration spectra are always higher than the SAC values especially for $T > 0.1$ sec, on the contrary the m+sd LSR spectrum matches not only the maximum value of the NS recorded spectra but also the shape, as can be seen from Fig. 13. This last figure shows in detail the comparison between the LSR spectrum (mean and m+sd), the SAC spectrum and the mean acceleration spectra of the recorded NS and EW components so as to highlight two important aspects: as previously discussed, the two horizontal components have different behaviour. The NS component reveals much higher values than the EW one and presents two noticeable peaks at 0.25 s and at 0.6 s. Therefore, the m+sd LSR spectrum is close both

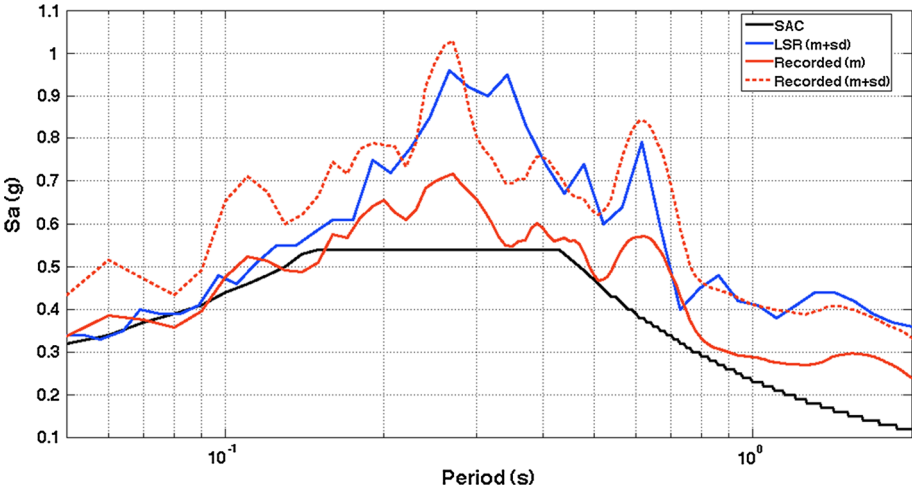


**Fig. 12** Comparison between the recorded acceleration spectra (in terms of mean and m+sd) with LSR and SAC approaches

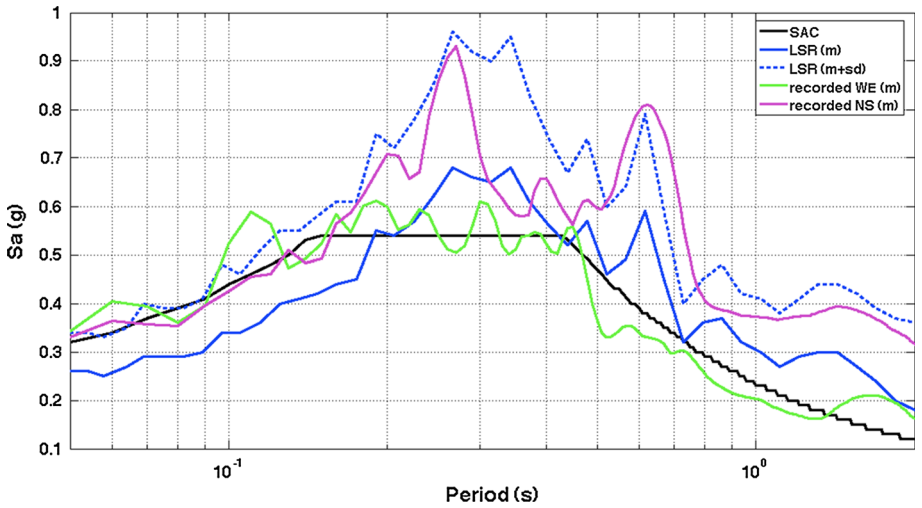


**Fig. 13** Comparison between the mean and m+sd deviation of LSR spectrum, SAC spectrum and the NS and EW components of the recorded acceleration spectra

to the maximum values and the shape of the NS recorded acceleration spectra, while the mean LSR spectrum is closer to the EW recorded acceleration spectra. The differences found between the NS and EW components show a clear directionality of the seismic motion. This directionality had significant effects on damage, as described in Liberatore et al. (2013) and Sorrentino et al. (2013).

Given the importance to consider the site effect as correctly as possible for the design of seismically safe buildings, the LSR approach provides more satisfactory results than the SAC one: the LSR has values much closer to the recorded ones up to 1 s especially for the NS recorded acceleration spectra. At present reliable estimates at longer periods ($T > 1$ s) cannot be obtained for two reasons: 1. we have no data at higher depths (i.e. $> 100$ m) possibly affecting the soil stratigraphy on the period range around/above 1 s; 2. since the MIRE station is very close to the earthquake fault, at longer periods the influence of permanent displacements is difficult to filter out of accelerograms with standard procedures without introducing possible spurious effects (no high-sampling-rate GPS recordings were available in the vicinity of the station to filter the data correctly). In general, even LSR response could fail to match exactly recorded earthquake spectra since no information is included as it concerns source directivity, crustal propagation (Malagnini et al. 2012) and amplification effects.

## 6 Conclusions

The strong ground motions recorded at several sites in the town of Mirandola, in the near field of the 2012 Emilia earthquakes, show some differences with respect to the code provision for that area considering the return periods of 475 years. Being aware that few recordings cannot be used to validate the PSHA estimates, we aimed at investigating how the observed differences depend on the ingredients of the code spectra that should be updated or modified in future issues of the NTC-2008 code.

There are generally differences according to the approach selected in order to take into account site effects. The Italian code states that local site response studies should be per-

formed, however spectra related to Vs30 classes and topography could be used as a simplified approach without giving indications on when/where this could be done.

For the Mirandola case, the presence of deep, soft soil deposits represents a clear situation in which the Vs30-class-based approach already proved to be inadequate in Italy (see Gallipoli and Mucciarelli 2009). This is confirmed when looking at the Vs30-class-based code spectra which are largely below the values observed, mostly in the NS recorded acceleration spectra.

On the other hand, the spectrum obtained convolving the bedrock code spectrum with the 1-D model of the first 100 m of soil provides a better agreement with the recordings (LSR approach). However, it has to be noted that the agreement obtained is satisfactory only in the frequency range corresponding to a quarter wavelength comparable with the depth of the available subsoil data. At lower frequencies the agreement is not good and, furthermore, a more detailed analysis of the observed spectra shows that there is complex, non-1D behaviour that could be due either to near source effects or complex propagation at depths larger than the one presently investigated.

**Acknowledgments** Marco Mucciarelli acknowledges the financial support of the Project SIGMA for the field work and geophysical survey. The work was greatly improved thanks to the suggestions of Fabio Sabetta and another anonymous reviewer.

## References

Albarello D, Cesi C, Eulilli V, Guerrini F, Lunedei E, Paolucci E, Pileggi D, Puzzilli LM (2011) The contribution of the ambient vibration prospecting in seismic microzoning: an example from the area damaged by the april 6, 2009 l'aquila (italy) earthquake. Boll Geof Teor Appl 52(3):513–538

Bordoni P, Azzara RM, Cara F, Cogliano R, Cultrera G, Di Giulio G, Fodarella A, Milana G, Pucillo S, Riccio G, Rovelli A, Augliera P, Luzi L, Lovati S, Massa M, Pacor F, Puglia R, Ameri G (2012) Preliminary results from emersito, a rapid response network for site-effect studies. Ann Geophys 55(4):599–607. doi:10.4401/ag-6153

Chiauzzi L, Masi A, Mucciarelli M, Vona M, Pacor F, Cultrera G, Gallovič F, Emolo A (2012) Building damage scenarios based on exploitation of housner intensity derived from finite faults ground motion simulations. Bull Earthq Eng 10(2):517–545

Crowley H, Stucchi M, Meletti C, Calvi GM, Pacor F (2009) Revisiting Italian design code spectra following the L'Aquila earthquake. Progettazione Sismica No 3/2009 Special Issue, IUSS PRESS (ISSN 1973-7432)

Decanini L, Mollaioli F, Oliveto G (2002) Structural and seismological implications of the 1997 seismic sequence in Umbria and Marche, Italy. In: Oliveto G (ed) Innovative approaches to earthquake engineering. WIT Press, Southampton, pp 229–323

Ditommaso R, Mucciarelli M, Gallipoli MR, Ponzo FC (2010) Effect of a single vibrating building on free-field ground motion: numerical and experimental evidences. Bull Earthq Eng 8:693–703. doi:10.1007/s10518-009-9134-5

Galli P, Castenetto S, Peronace E (2012) The MCS macroseismic survey of the Emilia 2012 earthquakes. Ann Geophys 55(4):663–672. doi:10.4401/ag-6163

Gallipoli MR, Mucciarelli M (2009) Comparison of site classification from VS30, VS10, and HVSR in Italy. Bull Seismol Soc Am 99:340–351

Gallipoli MR, Bianca M, Mucciarelli M, Parolai S, Picozzi M (2013) Topographic versus stratigraphic amplification: mismatch between code provisions and observations during the L'Aquila (Italy, 2009) sequence. Bull Earthq Eng 11:1325–1336. doi:10.1007/s10518-013-9446-3

GNDT Working Group (1999) Proposta di riclassificazione sismica del territorio nazionale. Ingegneria Sismica. XVI N.1, gennaio—aprile 1999 (in Italian)

Grimaz S, Malisan P (2013) Epicentral area effects and seismic hazard: a proposal for a multilayer hazard map (submitted to Boll Geof Teor Appl)

Gunay MS, Mosalam KM (2010) Structural engineering reconnaissance of the 6 April 2009. Abruzzo, Italy, Earthquake, and Lessons Learned. PEER report 2010/105. Pacific Earthquake Engineering Research Center, University of California, Berkeley

Housner GW (1952) Intensity of ground motion during strong earthquakes. Second technical report. August 1952, California Institute of Technology, Pasedena

Iervolino I (2012) Probabilità e salti mortali: le insidie della validazione della analisi di pericolosità attraverso l'occorrenza di singoli terremoti. Progettazione Sismica 2:37–43
Iervolino I, De Luca F, Chioccarelli E, Dolce M (2010) L'azione sismica registrata durante il mainshock del 6 aprile 2009 a L'Aquila e le prescrizioni del DM14/01/2008 V.1. Web report. http://www.reluis.it (in Italian)
Kottke AR, Rathje EM (2008) Technical manual for strata. PEER report 2008/10. Pacific Earthquake Engineering Research Center, University of California at Berkeley, February p 84
Liberatore L, Sorrentino L, Liberatore D, Decanini LD (2013) Failure of industrial structures induced by the Emilia (Italy) 2012 earthquakes. Eng Fail Anal. doi:10.1016/j.engfailanal.2013.02.009
Luzi L, Puglia R, Pacor F, Gallipoli MR, Bindi D, Mucciarelli M (2011) Proposal for a soil classification based on parameters alternative or complementary to Vs, 30. Bull Earthq Eng 9:1877–1898. doi:10.1007/s10518-011-9274-2
Malagnini L, Herrmann RB, Munafò I, Buttinelli M, Anselmi M, Akinci A, Boschi E (2012) The 2012 Ferrara seismic sequence: regional crustal structure, earthquake sources, and seismic hazard. Geophys Res Lett 39:L19302. doi:10.1029/2012GL053214
Martelli L, Calabrese L, Ercolessi G, et al (2013) Microzonazione sismica dell'area epicentrale del terremoto della pianura emiliana del 2012. XXXII Convegno GNGTS—Gruppo Nazionale di Geofisica della Terra Solida, 18–21 November 2013, Trieste, Italy (in Italian)
Masi A, Chiauzzi L, Braga F, Mucciarelli M, Vona M, Ditommaso R (2011) Peak and integral seismic parameters of L'Aquila, 2009 ground motions: observed vs code provision values. Bull Earthq Eng 9(1):139–156
Masi A, Vona M, Mucciarelli M (2011) Selection of natural and synthetic accelerograms for seismic vulnerability studies on RC frames. J Struct Eng 137(3):367–378
Masi A, Santarsiero G, Gallipoli MR, Mucciarelli M, Manfredi V, Dusi A, Stabile TA (2013) Performance of the health facilities during the 2012 Emilia earthquake and analysis of the Mirandola Hospital case study. Bull Earthq Eng (this issue). doi:10.1007/s10518-013-9518-4
Montaldo V, Meletti C, Martinelli F, Stucchi M, Locati M (2007) On-line seismic hazard data for the New Italian building code. J Earthq Eng 11(1):119–132
Mucciarelli M, Pacor F, Vanini M, Bettinali F (1997) Definition of seismic input for base isolation applications: methodologies assessment, statistical analysis and tools developed. In: Proceedings of the Post-SMIRT conference on Seismic Isolation, SMIRT, Taormina, Italy
NTC08 (2008) DM 14 gennaio 2008—Norme tecniche per le costruzioni. Ministero delle Infrastrutture. http://www.cslp.it (in Italian)
Ohori M, Nobata A, Wakamatsu K (2002) A comparison of ESAC and FK methods of estimating phase velocity using arbitrarily shaped micritremor arrays. Bull Seismol Soc Am 92:2323–2332
Okada H (2003) The microtremor survey method. Geophysical Monograph Series, SEG, 2003, p 129
Ordinanza del Presidente del Consiglio dei Ministri no. 3519/2006 (2006) Criteri generali per l'individuazione delle zone sismiche e per la formazione e l'aggiornamento delle medesime zone. Gazzetta Ufficiale 11 maggio 2006, No 108 (in Italian)
Parolai S, Richwalski SM, Milkereit C, Faeh D (2006) S-wave velocity profile for earthquake engineering purposes for the Cologne area (Germany). Bull Earthq Eng 4:65–94. doi:10.1007/s10518-005-5758-2
Pitilakis K, Riga E, Anastasiadis A (2013) New code site classification, amplification factors and normalized response spectra based on a worldwide ground-motion database. Bull Earthq Eng 11:925–966. doi:10.1007/s10518-013-9429-4
Priolo E, Romanelli M, Barnaba C, Mucciarelli M, Laurenzano G, Dall'Olio L, Abu Zeid N, Caputo R, Santarato G, Vignola L, Lizza C, Di Bartolomeo P (2012) The Ferrara thrust earthquakes of May-June 2012: preliminary site response analysis at the sites of the OGS temporary network. Ann Geophys 55(4):591–597. doi:10.4401/ag-6172
Sabetta F, Pugliese A (1996) Estimation of response spectra and simulation of nonstationary earthquake ground motions. Bull Seismol Soc Am 86(2):337–352
SESAME Project (2004) Guidelines for the implementation of the H/V spectral ratio technique on ambient vibrations. Measurements, processing and interpretation, WP12, deliverable No. D23.12, 2004. http://sesame-fp5.obs.ujf-renoble.fr/Papers/HV_User_Guidelines.pdf
Sorrentino L, Liberatore L, Liberatore D, Masiani R (2013) The behaviour of vernacular buildings in the 2012 Emilia earthquakes. Bull Earthq Eng. doi:10.1007/s10518-013-9455-2
Stucchi M, Meletti C, Montaldo V, Crowley H, Calvi GM, Boschi E (2011) Seismic hazard assessment (2003–2009) for the Italian building code. Bull Seismol Soc Am 101(4):1885–1911